PATH PLANNING FOR AUTOMATIC PARKING OF TRACTOR-TRAILER VEHICLES BASED ON BEZIER AND B-SPLINE CURVE MODELS

Fan LAI[1], Rui ZHU[2*], Shanqiu CHEN[3], Shibo BIN[4], Yongfei HAN[5], Zhao'an LIN[6], Liman WEI[7]

To address the challenges in path planning for automatic parking of tractor-trailer vehicles—such as complex trajectories, unstable path quality, and high modeling requirements—this study conducts a comparative analysis of Bezier and B-spline curve models under obstacle-free point-target parking scenarios. Performance evaluation is conducted based on geometric continuity, dynamic feasibility, and spatial efficiency. A novel three-segment hybrid path planning model is proposed by fusing second-order and third-order Bezier curves, effectively achieving the target parking task. The approach is validated through co-simulation using Simulink and TruckSim. Results show that the final planned trajectory reduces travel path length by up to 25.1% compared to single-curve models, with accurate heading angle control at the destination and minimum turning radius satisfying vehicle kinematic constraints. The proposed method overcomes limitations of conventional planning models and provides a theoretical foundation for the design and optimization of automatic parking systems for tractor-trailer vehicles.

Keywords: Tractor-Semitrailer, automatic parking, path planning, Bezier curve, B-Spline Curve

1. Introduction

In recent years, tractor-trailer vehicles have been widely adopted in logistics and transportation due to their high payload capacity, excellent transport efficiency, and low fuel consumption, becoming one of the core components of modern freight systems [1-3]. With the rapid development of smart logistics and intelligent control technologies, increasing attention has been paid to the intelligence level of tractor-trailers, especially in closed or semi-closed environments such as ports, industrial

[1] Lizhou Institute of Technology, Liuzhou, 545616, China
[2*] Liuzhou Institute of Technology, Liuzhou, 545616, China, email: 151727577@qq.com (corresponding author)
[3] Liuzhou Institute of Technology, Liuzhou, 545616, China
[4] Dongfeng Liuzhou Automobile Co., Ltd., Liuzhou, 545005, China
[5] Liuzhou Institute of Technology, Liuzhou, 545616, China
[6] Liuzhou City Vocational College, Liuzhou, 545036, China
[7] Dongfeng Liuzhou Automobile Co., Ltd., Liuzhou, 545005, China

parks, and mines, where the application prospects of autonomous driving technology are promising. Intelligent technologies not only help improve overall operational efficiency but also reduce driver workload and enhance the driving experience [4].

Parking is a critical operating scenario for vehicles, often facing challenges such as limited space and complex surroundings, which can easily lead to safety incidents. Achieving automated parking requires vehicles to possess high-precision path tracking capability and efficient obstacle avoidance strategies [5, 6]. A typical autonomous driving system consists of four main modules: perception, decision-making, planning, and control, among which path planning is a key component for realizing automated parking [7, 8]. For tractor-trailers, the tractor and trailer are connected via a hitch joint, resulting in asynchronous motion between the two units. This characteristic significantly increases the difficulty of path planning during reversing and parking maneuvers. Moreover, the large overall dimensions, high center of gravity, significant differences in wheelbase and trailer specifications, and complex matching of the distance between the tractor and trailer further exacerbate the challenges in path design.

To address these issues, researchers worldwide have proposed various path planning methods, primarily including:

(1) RRT (Rapidly-exploring Random Tree)-based methods and their improved variants, suitable for path search in high-dimensional unconstrained systems. For example, Chen et al. [9] and Ganesan et al. [10] applied the PSBi-RRT algorithm to autonomous parking of intelligent vehicles; Aydemir et al. [11] utilized the CL-RRT algorithm for autonomous navigation and reverse-path planning of mining trucks and trailers.

(2) Hybrid A* algorithm-based approaches, which extend traditional A* search by incorporating vehicle dynamics. For instance, Wei et al. [12] investigated backward path planning for semi-trailers using Hybrid A* combined with DP-RS curves.

(3) Quadratic Programming (QP) and optimization-based strategies, which formulate path planning as a constrained optimization problem. For example, Ben et al. [13] proposed a multi-objective integrated path planning method based on the NSGA-II algorithm; Asih et al. [14] and Ma'ruf et al. [15] employed genetic algorithms to construct a Green Vehicle Routing Problem (GVRP) model.

Despite providing new insights into tractor-trailer path planning, these methods still exhibit notable limitations: RRT-based approaches suffer from unstable path quality and low computational efficiency; Hybrid A* algorithms depend heavily on grid resolution and incur high computational costs; optimization-based methods are sensitive to initial solutions and involve high modeling complexity.

Therefore, this paper focuses on the fixed-point perpendicular parking task of tractor-trailer vehicles in obstacle-free environments. A systematic comparative analysis is conducted on the performance of second-order Bezier, third-order Bezier, and third-order B-Spline curve models. Furthermore, a novel three-segment path planning model that integrates second- and third-order Bezier curves is proposed, aiming to generate high-quality trajectories characterized by short path length, controllable heading angle, and curvature radius satisfying vehicle constraints. Finally, the effectiveness of the proposed method is validated through co-simulation using Simulink and TruckSim.

2. Vehicle Kinematic Model and Planning Task Description

2.1. Vehicle Kinematic Model Description

As shown in Figure 1, the kinematic model of a tractor-trailer system is established in a ground-fixed coordinate frame. Under low-speed operating conditions, the influence of vehicle dynamics is relatively small [16]. Therefore, the motion of the tractor can be described using a simplified single-track model, while the orientation of the trailer is determined by the motion of the tractor. In path planning, the primary focus is on the trajectory of the center line of the tractor.

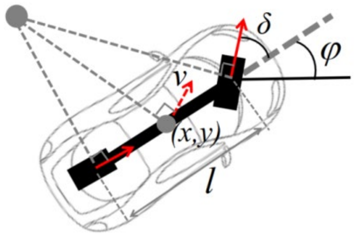

Fig. 1. Parameters of the vehicle kinematic model

In the ground-fixed coordinate system, the vehicle kinematic equations are described as follows:

$$\begin{bmatrix} \dot{x} \\ \dot{y} \\ \varphi \end{bmatrix} = \begin{bmatrix} cos\,\varphi \\ sin\,\varphi \\ \mathrm{tg}\delta/l \end{bmatrix} v \tag{1}$$

Where, (x, y) is the coordinate of the vehicle's rear axle center; φ is the vehicle's heading angle; δ is the front wheel steering angle; v is the rear axle speed; l is the wheelbase.

The vehicle can be regarded as a control system with input $u(v, \delta)$ and state vector $\chi(x, y, \delta)$, and its general form is:

$$\dot{\chi} = f(\chi, u) \tag{2}$$

The linear error model of the unmanned vehicle can be described as:

$$\dot{\tilde{\chi}} = \begin{bmatrix} \dot{x} - \dot{x}_r \\ \dot{y} - \dot{y}_r \\ \varphi - \dot{\varphi}_r \end{bmatrix} = \begin{bmatrix} 0 & 0 & -v\sin\varphi_r \\ 0 & 0 & v\cos\varphi_r \\ 0 & 0 & 0 \end{bmatrix} \begin{bmatrix} x - x_r \\ y - y_r \\ \varphi - \varphi_r \end{bmatrix} + \begin{bmatrix} \cos\varphi_r & 0 \\ \sin\varphi_r & 0 \\ tg\delta_r/l & v_r/(l\cos^2\delta_r) \end{bmatrix} \begin{bmatrix} v - v_r \\ \delta - \delta_r \end{bmatrix} \quad (3)$$

Where, $\dot{\tilde{\chi}}$ represents the difference between $\dot{\chi}$ and its reference value; r denotes the reference value; (x, y) is the coordinate of the vehicle's rear axle center; φ is the vehicle's heading angle; δ is the front wheel steering angle; v is the rear axle speed; l is the wheelbase.

A typical tractor-trailer consists of a tractor and a trailer connected by a hinge joint. To simplify the analysis and facilitate path planning, this paper adopts a simplified single-vehicle model to describe the motion of the tractor, with the trailer's posture determined by the motion of the tractor. Therefore, path planning primarily focuses on the center line trajectory of the tractor.

2.2. Planning Task Description

Tractor-trailer path planning is based on fundamental control theory. Starting from a given initial state, the vehicle follows a given or desired trajectory at a specified speed until reaching the destination. The schematic diagram of tractor-trailer path planning and trajectory tracking is shown in Figure 2.

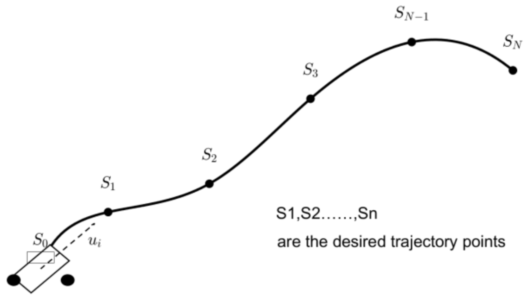

Fig. 2. Schematic diagram of tractor-trailer path planning and trajectory tracking

Perpendicular parking is a typical parking scenario for tractor-trailers, where the vehicle's initial parking position is usually perpendicular to the parking space. The path planning adopts a segmented design approach: the vehicle first drives to a certain point directly in front of the parking space, aligning the vehicle's center line with the center line of the parking space, after which it can move back straight into the spot. Typically, the turning radius of a tractor-trailer must be greater than 15 meters. The planning objective is to design a smooth path $r(t) = [x(t), y(t)]$ that guides the vehicle from the starting position to the endpoint of the first planning segment—where the vehicle's center line aligns with the parking space's center line. A schematic diagram of a typical perpendicular parking scenario for a tractor-trailer is shown in Figure 3. The parking scenario settings are described in Table 1.

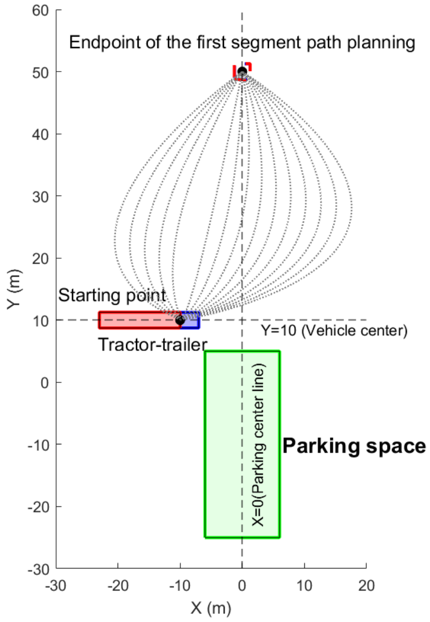

Fig. 3. Schematic Diagram of a Typical Perpendicular Parking Scenario for Tractor-Trailers.

Table 1

Settings for the Tractor-Trailer Perpendicular Parking Scenario

Item	Description
Starting Position	The tractor-trailer is located at the front-left of the parking space, with the center of the tractor's rear axle at coordinates$(x_s, y_s) = (-10,10)$,and starting heading angle$\phi_s = 0^{\circ}\sim 30^{\circ}$
Target Position	The tractor-trailer is located directly in front of the parking space, with the center of the tractor's rear axle at coordinates $(x_e, y_e) = (0,50)$,and ending heading angle$\phi_e = 90^{\circ} \pm 5^{\circ}$
Constraints	Minimum turning radiusR_{min}; The path must be a curve that is continuous and differentiable; Obstacle effects are not considered during path execution.

3. Construction and Optimization of Multiple Path Planning Curve Models

Path planning enables a vehicle to find an optimal route with the shortest distance from a starting point to a destination [17]. Automatic parking path planning is an essential computational step for achieving intelligent automated parking. Commonly used path planning curve models include Bezier curves, Hermite curves, polynomial curves, spirals, B-spline curves, and Pythagorean-Hodograph (PH) curves [18,19]. These curves typically possess good geometric continuity, allowing for the generation of smooth transition trajectories that effectively mitigate steering shocks. However, significant differences exist among these curve models in terms of expressive power, control degrees of freedom, computational complexity, and practical adaptability. There remains a lack of systematic research on how to select the most suitable path planning method under specific operating conditions.

This paper conducts a systematic comparative study on quadratic Bezier, cubic Bezier, and B-spline curves, based on the perpendicular parking path planning of a tractor-trailer in an obstacle-free environment.

3.1. Construction of the Quadratic Bezier Curve Model

The Bezier curve is derived from Bernstein polynomials and is widely used in research fields such as robot and aircraft path planning, with the advantage of continuous and controllable curvature [20]. The mathematical form of a quadratic Bezier curve is defined by three control points: the starting point P_0, the control point P_1, and the endpoint P_2. Its parametric equation is:

$$r(t) = (1-t)^2 P_0 + 2(1-t)tP_1 + t^2 P_2 \tag{4}$$

The expanded component form are:

$$\begin{aligned} x(t) &= (1-t)^2 x_0 + 2(1-t)tx_1 + t^2 x_2 \\ y(t) &= (1-t)^2 y_0 + 2(1-t)ty_1 + t^2 y_2 \end{aligned} \tag{5}$$

The forms of its first and second derivatives are:

$$\begin{aligned} \dot{x}(t) &= 2(1-t)(x_1 - x_0) + 2t(x_2 - x_1) \\ \dot{y}(t) &= 2(1-t)(y_1 - y_0) + 2t(y_2 - y_1) \\ \ddot{x}(t) &= 2(x_2 - 2x_1 + x_0) \\ \ddot{y}(t) &= 2(y_2 - 2y_1 + y_0) \end{aligned} \tag{6}$$

The curvature formula is:

$$\kappa(t) = \frac{|\dot{x}\ddot{y} - \dot{y}\ddot{x}|}{(\dot{x}^2 + \dot{y}^2)^{3/2}} \tag{7}$$

When using a quadratic Bezier curve for path planning, since the positions of the start point P0 and the end point P_2 are fixed, the path can be adjusted by modifying the position of the control point P1. The search range for the control point P1 is $x \in [-10,15]$,$y \in [5,50]$.

To obtain the optimal quadratic Bezier curve, this paper adopts a trial-and-error method combined with a numerical search approach to select six coordinates(x,y)= (-5,10), (-5,20), (0,20), (5,30), (10,30), (10,35) for the control point P1 specifically for numerical model analysis of the response curves. The comparison of the response curves is shown in Figure 4.

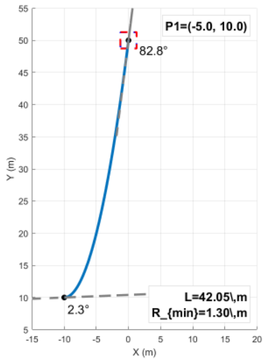

Scheme1:P1= (-5,10)

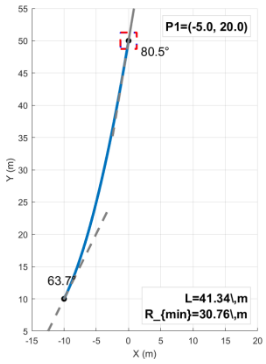

Scheme2:P1= (-5,20)

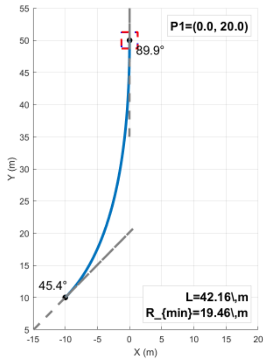

Scheme3:P1= (0,20)

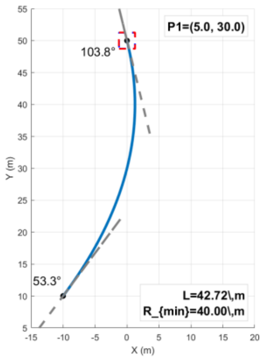

Scheme4:P1= (5,30)

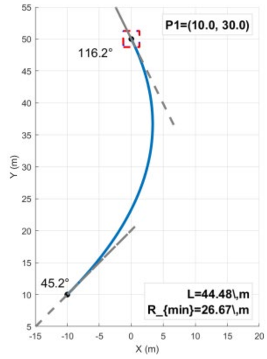

Scheme5:P1= (10,30)

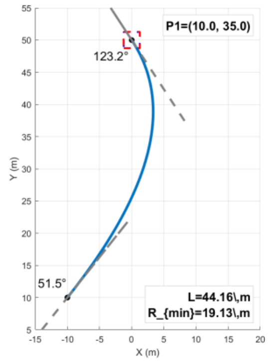

Scheme6:P1= (10,35)

Fig. 4. Comparison of response curves for different P_1 positions

Data analysis reveals the following: When P_1 = (-5, 10), the path exhibits severe bending at the initial segment, with a minimum curvature radius Rmin of only 1.30 m, far below the typical minimum turning radius for a tractor-trailer. When P_1 = (-5, 20), the path length L is the shortest at 41.34 m, but the deviation at the endpoint direction is significant. When P_1 = (0, 20), the overall path is smooth, with Rmin reaching 19.46 m, and the ending heading angle (ϕ_e) satisfies the perpendicular target direction; however, it suffers from an excessively large starting heading angle (ϕ_s)and a non-optimal path length. When P_1 = (5, 30), Rmin is maximized at 40.00 m, but the path length correspondingly increases. As P_1 continues to move further to the upper right, Rmin begins to decrease again while the path length increases. Since the quadratic Bezier curve has only one intermediate control point, it cannot independently control the tangent directions at both ends, making it difficult to precisely control the heading angles in path planning.

3.2. Construction of the Cubic Bezier Curve Model

As the order of the Bezier curve increases, its fitting accuracy improves. However, when the order exceeds four, overfitting can occur. Compared to the quadratic Bezier, the cubic Bezier introduces four control points, enabling more precise curve control. In addition to the start and end points, the two intermediate control points P_1 and P_2 can be reasonably set to precisely control the degree of path curvature and transition characteristics. A comparison between the quadratic and cubic Bezier curve models is shown in Figure 5.

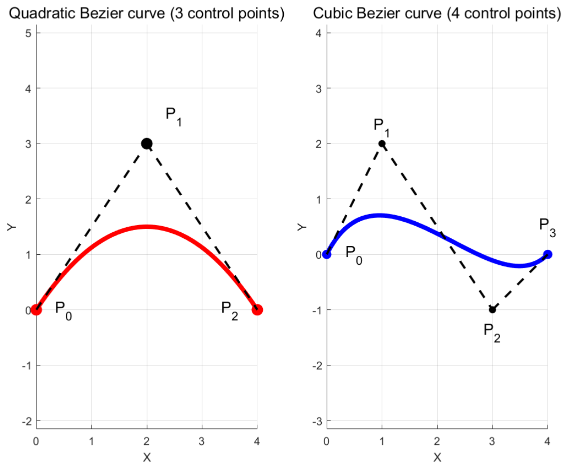

Fig. 5. Comparison between the quadratic Bezier and cubic Bezier models

The parametric equation of the cubic Bezier curve can be expressed as:

$$r(t) = (1-t)^3 P_0 + 3(1-t)^2 t P_1 + 3(1-t)t^2 P_2 + t^3 P_3 \quad (8)$$

The expanded component form are:

$$x(t) = (1-t)^3 x_0 + 3(1-t)^2 t x_1 + 3(1-t)t^2 x_2 + t^3 x_3$$
$$y(t) = (1-t)^3 y_0 + 3(1-t)^2 t y_1 + 3(1-t)t^2 y_2 + t^3 y_3 \quad (9)$$

The forms of its first and second derivatives are:

$$\dot{r}(t) = 3(1-t)^2(P_1 - P_0) + 6(1-t)t(P_2 - P_1) + 3t^2 P_2 + t^3(P_3 - P_2) \quad (10)$$
$$\ddot{r}(t) = 6(1-t)(P_2 - 2P_1 + P_0) + 6t(P_3 - 2P_2 + P_1)$$

When constructing a path curve model using a cubic Bezier curve, the planned path can be parameter-optimized by iteratively adjusting the coordinates of control points P_1 and P_2. By introducing virtual arc length parameters L_1 and L_2, the relative positions and distances of P_1 and P_2 with respect to the start and end points can be more intuitively expressed. In this analysis, the optimization variables are defined as $u = [x_1, y_1, x_2, y_2]^T$. Based on different L_1 and L_2 length parameters, ten combination schemes are designed for comparative analysis of the cubic Bezier curve. The comparison results of minimum turning radius and path length for each scheme are shown in Table 2. The data show that the curvature radius increases with increasing L_1, but none of the schemes achieve the required 15 m. The maximum curvature radius is only 9.78 m (Scheme 8). Additionally, as L_1 increases, the path length also increases.

Table 2

Analysis Results Data for Each Scheme

No.	L_1	L_2	P_1 (x_1, y_1)	P_2 (x_2, y_2)	Curvature Radius /m	Path Length /m
1	1	1	(-9, 10)	(0, 49)	0.04	41.29
2	5	5	(-5, 10)	(0, 45)	1.08	42.03
3	10	10	(0, 10)	(0, 40)	4.59	43.61
4	15	15	(5, 10)	(0, 35)	8.00	45.68
5	20	20	(10, 10)	(0, 30)	7.94	48.15
6	25	25	(15, 10)	(0, 25)	6.02	50.96
7	30	30	(20, 10)	(0, 20)	4.04	54.09
8	25	10	(15, 10)	(0, 40)	9.78	49.62
9	20	15	(10, 10)	(0, 35)	8.87	47.73
10	20	10	(10, 10)	(0, 40)	9.43	47.37

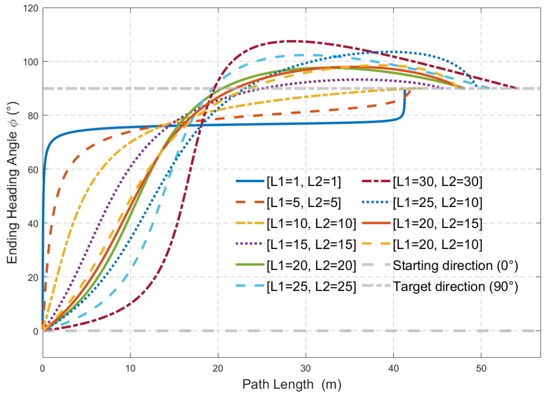

Fig. 6. Comparison curves of heading angles for each scheme

Figure 6 shows the comparison curves of the heading angles for each scheme as they vary with the control points. It can be seen that the heading angles at the end point of all schemes tend towards the target requirement of 90° . This is due to the setting of the virtual arc length L2. Moreover, as L2 increases, the curves become more upward, leading to a more stable control of the heading angle at the endpoint.

3.3. B-Spline Curve Model Construction

The B-Spline curve is constructed based on known data points. A knot vector is generated using the uniform parameterization method, from which the basis functions are derived. Subsequently, a diagonal matrix is formed using an approximation approach, and the control points are solved using the Thomas algorithm (tridiagonal matrix algorithm). Finally, curve fitting is performed [21].

The B-Spline is a piece-wise polynomial curve, and its equation can be expressed as

$$r(t) = \sum_{i=0}^{n} N_{i,k}(t) P_i \tag{11}$$

Where, $N_{i,k}(t)$ is the i-th k-th order B-spline basis function, Pi is the control point, and the knot vector $T = \{t_0, t_1, \dots \dots t_m\}$ determines the support interval of the basis function.

Based on the given control points, the response curves of B-Splines with different orders are shown in Figure 7. It can be seen that as the order increases, there is no significant change in the B-Spline response curves, but the computational load increases. For this analysis, a cubic (third-order) B-Spline model is selected.

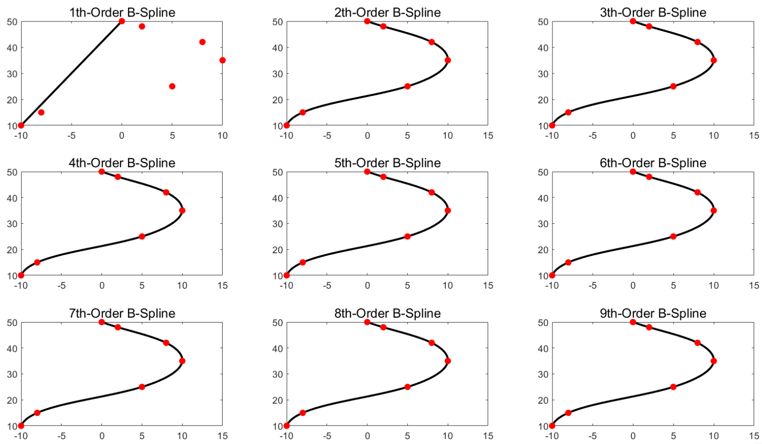

Fig. 7. Response curves of B-Splines with different orders (based on given control points)

For a cubic B-Spline, the order k is 4, and a uniform knot vector is used:

$$t_i = \frac{i}{m-k}, i = 0,1, \dots \dots m \tag{12}$$

Calculate the curve control points using the recursive formula:

$$P_i^{(0)} = P_i, P_i^{(r)} = (1-\alpha)P_{i-1}^{(r-1)} + \alpha P_i^{(r-1)}$$

$$\alpha = \frac{t - t_{i+k-r}}{t_{i+1} - t_{i+k-r}} \tag{13}$$

A cubic B-Spline typically uses 5 to 6 control points. Excluding the start and end points, usually 3 to 4 intermediate control points are set to approximate the desired path. This paper selects 5 control points and proposes 6 analysis scheme combinations as follows:

X-coordinates for each scheme:		Y-coordinates for each scheme:
Scheme 1:	[-10, -6, 2, 1, 0];	[10, 20, 35, 45, 50];
Scheme 1:	[-10, -7, 1, 3, 0];	[10, 14, 28, 42, 50];
Scheme 1:	[-10, -4, 5, 2, 0];	[10, 18, 36, 46, 50];
Scheme 1:	[-10, -5, 4, 6, 0];	[10, 16, 30, 44, 50];

Scheme 1: [-10, -6, 3, 1, 0]; [10, 16, 32, 45, 50];
Scheme 1: [-10, -5, 3, 0.5, 0]; [10, 15, 30, 45, 50];

Numerical analysis was performed on each scheme, and the comparative data of minimum curvature radius and path length are shown in Figure 8. It can be seen that only Scheme 2 satisfies the constraint requirements, with a minimum turning radius of 17.79 m and a path length of 44.08 m.

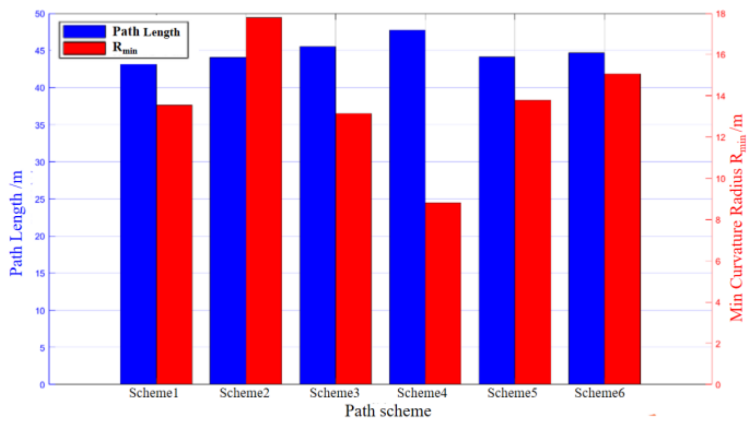

Fig. 8. Bar chart comparison of path length and minimum curvature radius for each scheme

3.4. Construction of a Hybrid Curve Model Combining Quadratic and Cubic Bezier Curves

Based on the above analysis, it is found that for the path planning of tractor-trailers under the given conditions: the quadratic Bezier curve model achieves the shortest path length and favorable curvature radius characteristics, but struggles to precisely control heading angles; the cubic Bezier model allows accurate control of heading angles at both start and end points, yet results in a relatively small curvature radius; while the cubic B-Spline model tends to generate paths with excessive length. Therefore, by fusing the quadratic and cubic Bezier curve models, it is possible to achieve optimal control of heading angles while simultaneously realizing favorable path length and curvature radius characteristics.

The construction concept for the hybrid model of quadratic and cubic Bezier curves is as follows: the planned path is divided into three segments. The curve models and control points for each segment are shown in Table 3. Here, P_0 is the starting point, P_3 is the endpoint, J_1 is the end point of the first segment (and start point of the second segment), J_2 is the end point of the second segment (and start point of the third segment), C_1 and $C_2$are the control points for the first segment, C_m is the control point for the second segment, and C_3 and C_4 are the control points for the final segment.

Table 3

Curve Model and Control Point Settings for Each Segment

Segment	Type	Control Points
Segment 1	Cubic Bezier	P_0, C_1, C_2, J_1
Segment 2	Quadratic Bezier	J_1, C_m, J_2
Segment 3	Cubic Bezier	J_2, C_3, C_4, P_3

Based on the parametric equations and derivative expressions of the quadratic Bezier and cubic Bezier curves mentioned earlier, to ensure continuity of the curve at points J_1 and J_2, these points must satisfy the tangent continuity condition. That is:

At point J_1:

$$3(J_1 - C_2) = 2(C_m - J_1) \Rightarrow C_m = \frac{3}{2}(J_1 - C_2) + J_1 \quad (14)$$

At point J_2:

$$2(J_2 - C_m) = 3(C_3 - J_2) \Rightarrow C_3 = \frac{2}{3}(J_2 - C_m) + J_2 \quad (15)$$

The combined curve model after fusing the quadratic Bezier and cubic Bezier curves, along with the correlation characteristics of each control point, is illustrated in Figure 9.

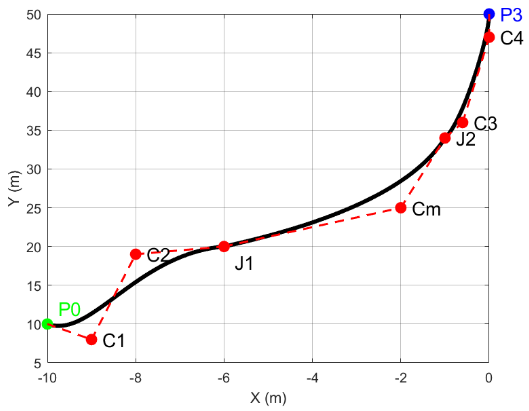

Fig. 9. Hybrid curve model combining quadratic and cubic Bezier curves

Based on the parking boundary conditions for the tractor-trailer given in this analysis, different path planning results can be obtained by adjusting different sets of control point coordinates using the hybrid model of quadratic and cubic Bezier curves. Three schemes with different control point coordinate sets were designed, and the corresponding response curves are shown in Figure 10. It can be seen that Scheme 2 is the optimal solution, as it satisfies the requirements for heading angles at the start and end points, meets the minimum curvature radius constraint, and achieves a relatively favorable path length.

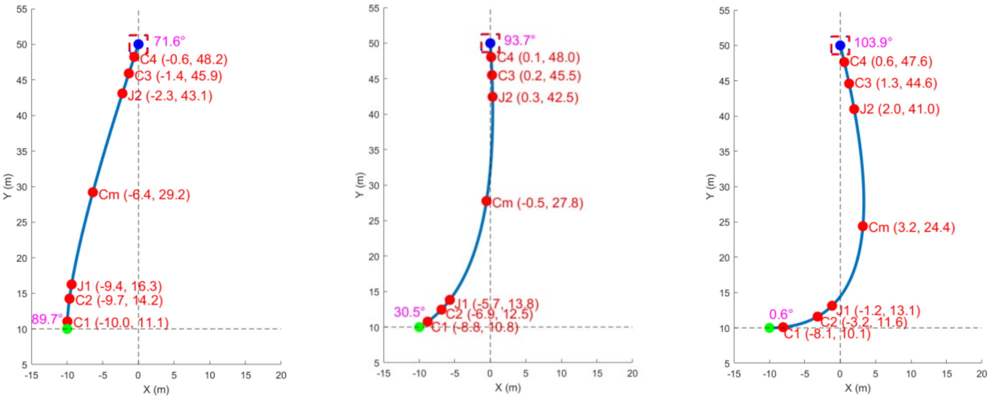

Scheme1 Scheme2 Scheme3

Fig. 10. Control point coordinate sets and response curves for the hybrid schemes

4. Co-simulation Verification using Simulink and TruckSim

Based on the optimal planned path obtained from the previous analysis, a co-simulation model integrating Simulink and TruckSim was established to verify the feasibility of the proposed path planning scheme.

4.1. Simulation Platform Setup

Commonly used path tracking control methods in intelligent vehicles include Model Predictive Control (MPC), Proportional-Integral-Derivative (PID) control, sliding mode control, and Linear Quadratic Regulator (LQR) control [22]. In this study, a tractor-trailer automated parking control system model is developed based on a nonlinear MPC control algorithm. The system inputs the desired target pose, path weighting parameters (Qp, Rp, Qt, Rt), and the distance between the vehicle and the centerline of the parking space into the MPC controller, enabling optimized solutions for path following and steering angle. The control outputs from the controller are transmitted to the vehicle model via the simulation interface Truck S-Function. A closed-loop feedback mechanism then corrects the vehicle's motion state, ultimately achieving accurate path tracking for the tractor-trailer. The completed co-simulation model is shown in Figure 11.

In TruckSim, a tractor-trailer model consisting of a two-axle tractor and a single-axle trailer is imported. The road friction coefficient is set to 0.85, the vehicle speed is set to 10 km/h, and the path tracking duration is 20 seconds.

4.2. Coupling Analysis Results

After completing the model setup, a coupling analysis was carried out. The results of the coupling analysis were extracted to plot the vehicle's travel trajectory and the swept area of the vehicle body's outer contour, as shown in Figure 12. It can be seen that the length L of the travel trajectory along the planned path is 40.5 m, which is a maximum reduction of 25.1% compared to the length of the single-curve model's planned path. The minimum turning radius Rmin is 15.06 m, satisfying the requirement for minimizing the minimum turning radius. The ending heading angle (ϕ_e) is 90.5°, achieving the precise control objective of the terminal heading angle.

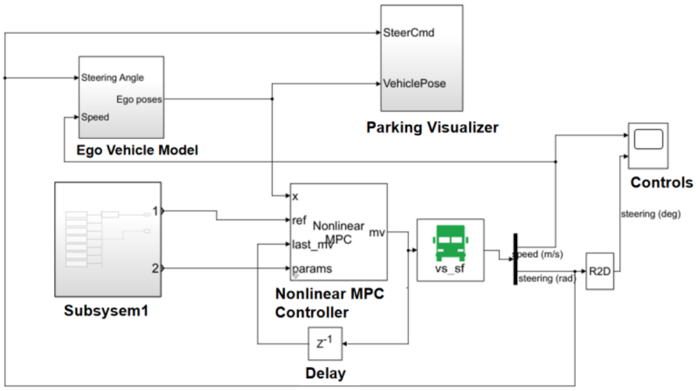

Fig. 11. Setup of the co-simulation model using Simulink and TruckSim

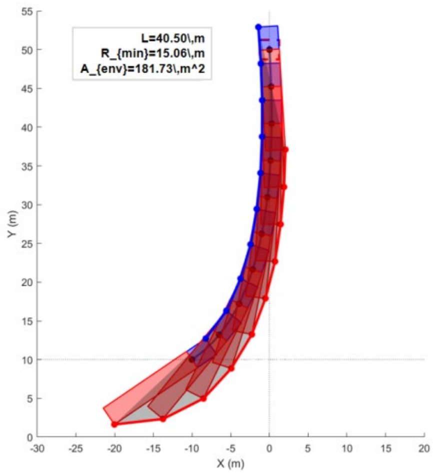

Fig. 12. Vehicle Travel Trajectory and Swept Area of the Coupled Model

5. Conclusion

This paper systematically investigates the performance of three path planning models—quadratic Bezier, cubic Bezier, and cubic B-Spline—for the task of fixed-point perpendicular parking of tractor-trailers in obstacle-free environments. A three-segment path planning method that fuses quadratic and cubic Bezier curves is proposed. The main conclusions are as follows:

(1) Single-curve models exhibit significant limitations in tractor-trailer parking path planning: the quadratic Bezier struggles to control heading angles, the cubic Bezier tends to produce longer paths with potentially excessive curvature, and the B-Spline model results in long path lengths and complex optimization.

(2) The proposed hybrid model, through a segmented design, effectively balances path length, curvature characteristics, and heading angle control accuracy, thereby significantly enhancing the overall performance of path planning.

(3) Co-simulation results verify the feasibility of the proposed method: compared to single-curve models, the path length is reduced by up to 25.1%, the terminal heading angle is precisely controlled, and the minimum turning radius satisfies vehicle dynamic constraints.

In summary, the proposed Bezier hybrid curve model provides an efficient and feasible solution for path planning in tractor-trailer automated parking, demonstrating strong potential for practical engineering applications.

Acknowledgement

1. 2024 Guangxi University Young and Middle-Aged Teachers' Scientific Research Basic Ability Improvement Project "Research on Path Planning and Tracking Control for Tractor-Trailer Automatic Parking Systems" (2024KY1810);

2. Liuzhou Institute of Technology: Guangxi Higher Education Engineering Research Center for Intelligent Control of New Energy Vehicles;

3. 2023 Guangxi University Young and Middle-Aged Teachers' Scientific Research Basic Ability Improvement Project "Simulation Research on Lane Keeping and Rollover Stability Control Based on Commercial Vehicles" (2023KY1775).

REFERENCES

[1] *Hoang, N.T., Nguyen, H.V., Le, N.D., Ho, H.H. and Nguyen, T.L.* (2025) 'Artificial potential field based motion planning for autonomous tractor-trailer vehicles', Results in Engineering, 27, doi:10.1016/j.rineng.2025.105936

[2] *Ritzen, P., Roebroek, E., van de Wouw, N., Jiang, Z.-P. and Nijmeijer, H.* (2016) 'Trailer steering control of a tractor–trailer robot', IEEE Transactions on Control Systems Technology, 24, pp. 1240–1252.

[3] *Kayacan, E., Ramon, H. and Saeys, W.* (2014) 'Distributed nonlinear model predictive control of an autonomous tractor–trailer system', Mechatronics, 24, pp. 926–933.

[4] *Siddiqi, M.R., Saharkhiz, A., Milani, S., Fu, C., Jazar, R.N. and Marzbani, H.* (2022) 'Analysis for comfortable handling and motion sickness minimization in autonomous vehicles using ergonomic path planning with cost function evaluation', SAE International Journal of Commercial Vehicles, 5, pp. 147–163.

[5] *Kim, W.J., Lee, Y.J., Ahn, W.J., Lim, M.T. and Pac, D.S.* (2025) 'Adaptive vehicle path planning in alleyway using looming ODG-MPC', International Journal of Control, Automation, and Systems, 23, pp. 2219–2231.

[6] *Macioszek, E.* (2018) 'First and last mile delivery—problems and issues', in Proceedings of Advanced Solutions of Transport Systems for Growing Mobility: 14th Scientific and Technical Conference "Transport Systems. Theory & Practice 2017" Selected Papers. Cham: Springer, pp. 147–154.
[7] *Li, T., Ren, H. and Li, C.* (2024) 'Intelligent electric vehicle trajectory tracking control algorithm based on weight coefficient adaptive optimal control', Transactions of the Institute of Measurement and Control, 46, pp. 2647–2663.
[8] *Cao, L.L., Liu, W., Dai, K.P. and Zhou, G.F.* (2024) 'Path tracking control of autonomous tractor-trailer vehicles based on corner compensation LQR', Journal of Automotive Safety and Energy Conservation, 15, pp. 413–423.
[9] *Chen, J., Ma, R., Lu, C. and Deng, Y.* (2025) 'Autonomous parking path planning method for intelligent vehicles based on improved RRT algorithm', World Electric Vehicle Journal, 16, pp. 374–394.
[10] *Ganesan, S., Ramalingam, B. and Mohan, R.E.* (2024) 'A hybrid sampling-based RRT* path planning algorithm for autonomous mobile robot navigation', Expert Systems with Applications, 258(000):12, doi:10.1016/j.eswa.2024.125206
[11] *Aydemir, E. and Unel, M.* (2025) 'Motion planning and path following for autonomous navigation and reversing of a full-scale mining truck and trailer system', International Journal of Automotive Technology, 26, pp. 595–606.
[12] *Wei, J.Q., Tang, S.J., Du, W.Z. and Deng, G.F.* (2025) 'Semi-trailer reverse path planning based on hybrid A and DP-RS curve', Modern Electronics Technique, available at: https://link.cnki.net/urlid/61.1224.tn.20250603.0941.002.
[13] *Ben Abbes, S., Rejeb, L. and Baati, L.* (2022) 'Route planning for electric vehicles', IET Intelligent Transport Systems, 16, pp. 875–889.
[14] *Asih, H.M., Leuveano, R.A.C., Dharmawan, D.A. and Ardiansyah, A.* (2025) 'Genetic algorithm to optimize green vehicle routing and allocation planning for perishable products', International Journal of Advances in Intelligent Informatics, 11, pp. 175–191.
[15] *Ma'ruf, A. and Budhiarti, D.* (2024) 'Development of genetic algorithm for human-robot collaboration assembly line design', International Journal of Industrial Optimization, 5, pp. 118–133.
[16] *Gong, J.W., Liu, K. and Qi, J.Y.* (2023) Unmanned vehicle model predictive control (2nd ed.). Beijing: Beijing Institute of Technology Press.
[17] *Wang, H.Q., Gan, C.T. and Wang, F.B.* (2025) 'Path planning for unmanned vehicles using improved A algorithm', Journal of Machinery Design and Manufacture, 1, pp. 117–120.
[18] *Li, Z.C., Li, J.Q. and Wang, W.C.* (2023) 'Path planning and obstacle avoidance control for autonomous multi-axis distributed vehicle based on dynamic constraints', IEEE Transactions on Vehicular Technology, 72, pp. 4342–4356.
[19] *Hoek, R.V., Ploeg, J. and Nijmeijer, H.* (2021) 'Cooperative driving of automated vehicles using B-splines for trajectory planning', IEEE Transactions on Intelligent Vehicles, 6, pp. 594–604.
[20] *Chen, T., Cai, Y.F., Chen, L. and Xu, X.* (2025) 'Trajectory planning method for emergency rescue vehicles based on fourth-order Bézier curves', Journal of Mechanical Engineering, 61, pp. 198–209.
[21] *Wang, J.X., Zhuang, J.H., Cheng, X.M., Huang, L., Xie, P.C. and Yan, Y.* (2020) 'MPC trajectory re-planning algorithm under B-spline curves', Journal of Chongqing University of Technology (Natural Science), 34, pp. 27–35.
[22] *Huang, L., Chen, Q.P., Jiang, Z.Q., Zhang, Y., Li, Y. and Liu, H.* (2025) 'Intelligent automobile path tracking control based on T-S fuzzy controller', Transactions of the Institute of Measurement and Control, 47, pp. 1081–1090.